AN ABSTRACT OF THE THESIS OF

William Howard Zimmerman (Name) for the M.S. (Degree) in Mechanical Engineering (Major)

Date thesis is presented August 29, 1966

Title THE DESIGN OF A PHOTOELASTIC LOAD CELL

Redacted for privacy

Abstract approved ____ (Major Professor) ____

This work shows how a new design in a load cell can be built using the principles of photoelasticity. From photoelasticity one knows that fringes denoting the stress pattern can be observed in a plastic model viewed in a polariscope. Through knowledge of the properties of the material one can determine the load necessary to produce a certain fringe. Two photocells can be used to measure the change in the fringe order. One photocell is used as a reference while the other photocell observes the changing light intensity, coming through a miniature polariscope, caused by the stress pattern. This difference in light intensity can be displayed on a meter which is calibrated to give a reading of the applied load. The stress optic constant varies for the different photoelastic materials giving the load cell several ranges of loading. Also, model size may be varied, giving additional selectivity in the range of loading while keeping the accuracy high. Load ranges may range from 0-2.7 ounces to 0-430 pounds. The load cell is easily calibrated by using dead weights.

It is felt that this study has met the need of finding a low cost method of measuring small loads with relatively high accuracy.

THE DESIGN OF A PHOTOELASTIC LOAD CELL

by

WILLIAM HOWARD ZIMMERMAN

A THESIS

submitted to

OREGON STATE UNIVERSITY

in partial fulfillment of
the requirements for the
degree of

MASTER OF SCIENCE

June 1967

APPROVED:

Redacted for privacy

Professor of Mechanical Engineering
In Charge of Major

Redacted for privacy

Chairman of Department of Mechanical Engineering

Redacted for privacy

Dean of Graduate School

Date thesis is presented

Typed by Donna Olson

TABLE OF CONTENTS

LIST OF FIGURES

LIST OF TABLES

THE DESIGN OF A PHOTOELASTIC LOAD CELL

I. INTRODUCTION

Statement of the Problem

There is an ever growing need for a compact, accurate method of measuring forces at moderate cost. The forces to be concerned with are in the range of 0 to 50 pounds. Thus, a load cell that is sturdy and easy to use combined with the above features is desired for student use.

A load cell is a device which produces an output signal proportional to the applied load or force. This means that a commercially available load cell with a range of 0 to 25 pounds and 2% accuracy full scale will give a reading proportional to the true force $\pm$ the error involved. The load cell sought in this study should retain high accuracy at any loading.

Purpose of the Study

The purpose of this study was to design and test a load cell with such desired characteristics by using the principles of photoelasticity. Through the application of these principles in conjunction with one's knowledge of photocells in a somewhat unique manner, the above problem has been solved in a satisfactory way.

The proposed and tested design can be built for a cost of approximately $15 and uses readout equipment that is usually found in most laboratories or can be purchased for under $35. This is considerably cheaper than commercially available load cells costing from $245 to $325 for a similar range. Then the readout equipment may cost an additional $545 to $745.

II. ELEMENTARY ELASTICITY

Whenever loads are applied to a solid body such as a beam or some other part of a structure, stresses are set up in the body which may vary from point to point. The magnitude and direction of the stress at a point depends upon the loads applied and also upon the shape of the body. This study is concerned with a force or a load on some type of structure; thus, it is concerned with stress and it is for this reason that some background in elasticity must be considered.

There are two basic types of force that produce stress on a body (3, p. 4). They are surface and body forces. Surface forces occur when one body comes in contact with another body. The forces are applied at the surfaces of the bodies. The second type of force, being called body force, pertains to each element of the body. Body forces are usually produced by gravitational, centrifugal, or other force fields. Body forces for many practical applications may be considered of negligible importance and neglected without introducing serious error.

This study will be concerned with stresses and strains in two dimensions at a point. "The term stress denotes force per unit area" (6, p. 1). Stress σ acting at a point P over area ΔA may be defined by the expression (8, p. 62-66)

$$\sigma = \underset{\Delta A \to 0}{\text{Limit}} \frac{\Delta F}{\Delta A} = \frac{dF}{dA}$$

where ΔF denotes the increment of force acting on the area ΔA about the point P. The stress σ is for convenience resolved into normal and shear stresses which are respectively normal and parallel to the area ΔA. The above equation may be written for the simple case as $\sigma = \frac{F}{A}$ (9, p. 5).

Often, to apply mathematical formulas, a modification to the solution of boundary value problems in elasticity must be used. An approximation such as this may be valid if it satisfies Saint-Venant's Principle (18, p. 33), which states that if a system of external forces acting on a body is replaced by another system of forces acting on the same body with the same effect, the distribution of stresses and strains in the body will not be changed appreciably except in the vicinity of the application of the forces. The body is assumed to be made of a homogeneous material and continuous throughout. The body is also assumed to be isotropic everywhere. Assume that a straight tension bar as shown in Figure 1 is loaded in pure tension. In Figure 2 consider the free body diagram; this simple case is calculated as: (9, p. 5)

$$\sigma = \frac{F}{A}$$

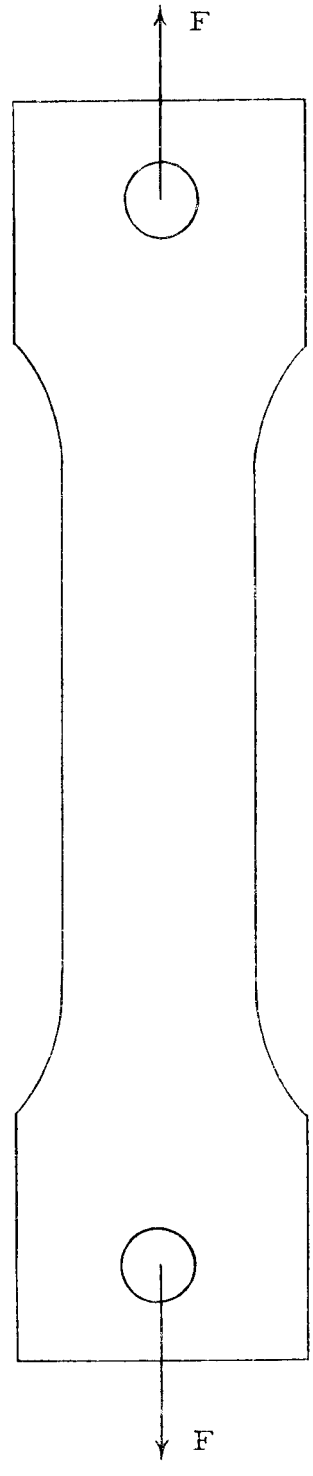

Figure 1. Simple tension model.

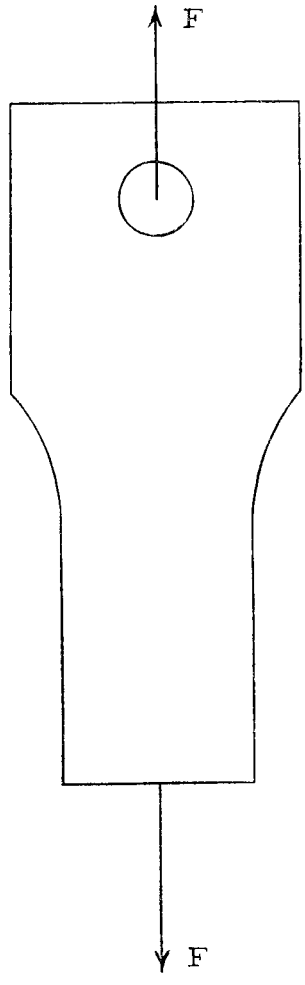

Figure 2. Force equilibrium.

where

F = tensile force

A = cross-sectional area of the bar

However, if a section other than perpendicular to the axis of the bar is taken as in Figure 3 there must be a shearing stress $\tau = \frac{T}{A}$ as well as the normal stress $\sigma = \frac{N}{A}$. Thus, for the two-dimensional case there is a biaxial state of stress. This may be represented at a point by the stresses acting on an element as shown in Figure 4. Consider again Figure 3, applying the equation of equilibrium to the free-body diagram for forces in the normal direction. The expression: (9, p. 17-19)

$$F \cos\theta = N = \frac{\sigma A}{\cos\theta}$$

is obtained which can be put in the form:

$$\sigma = \frac{F}{A} \cos^2\theta = (\frac{F}{2A})(1+\cos 2\theta)$$

Similarly in the tangential direction

$$F \sin\theta = T = \frac{\tau A}{\cos\theta}$$

$$\tau = (F/A) \sin\theta \cos\theta = (F/2A) \sin 2\theta.$$

These equations may now be plotted to give the curves shown in Figure 5. From this graph it can be seen that σ is a maximum

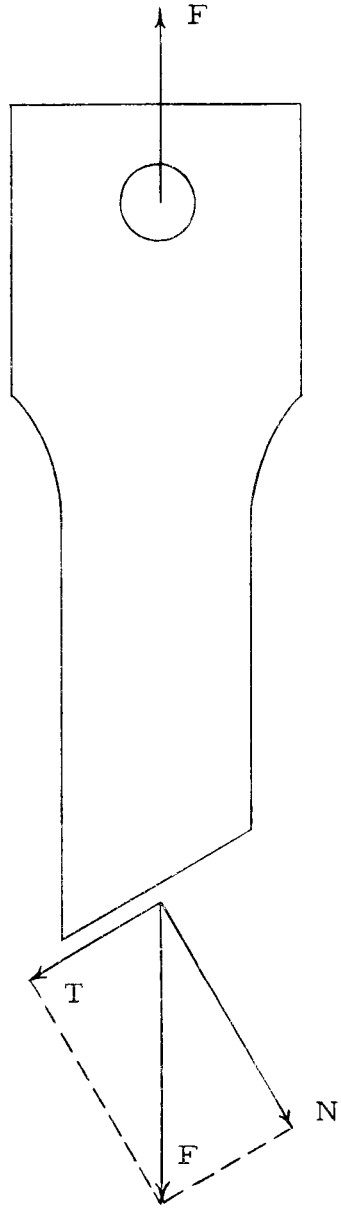

Figure 3. Vector representation of forces acting on a nonperpendicular section.

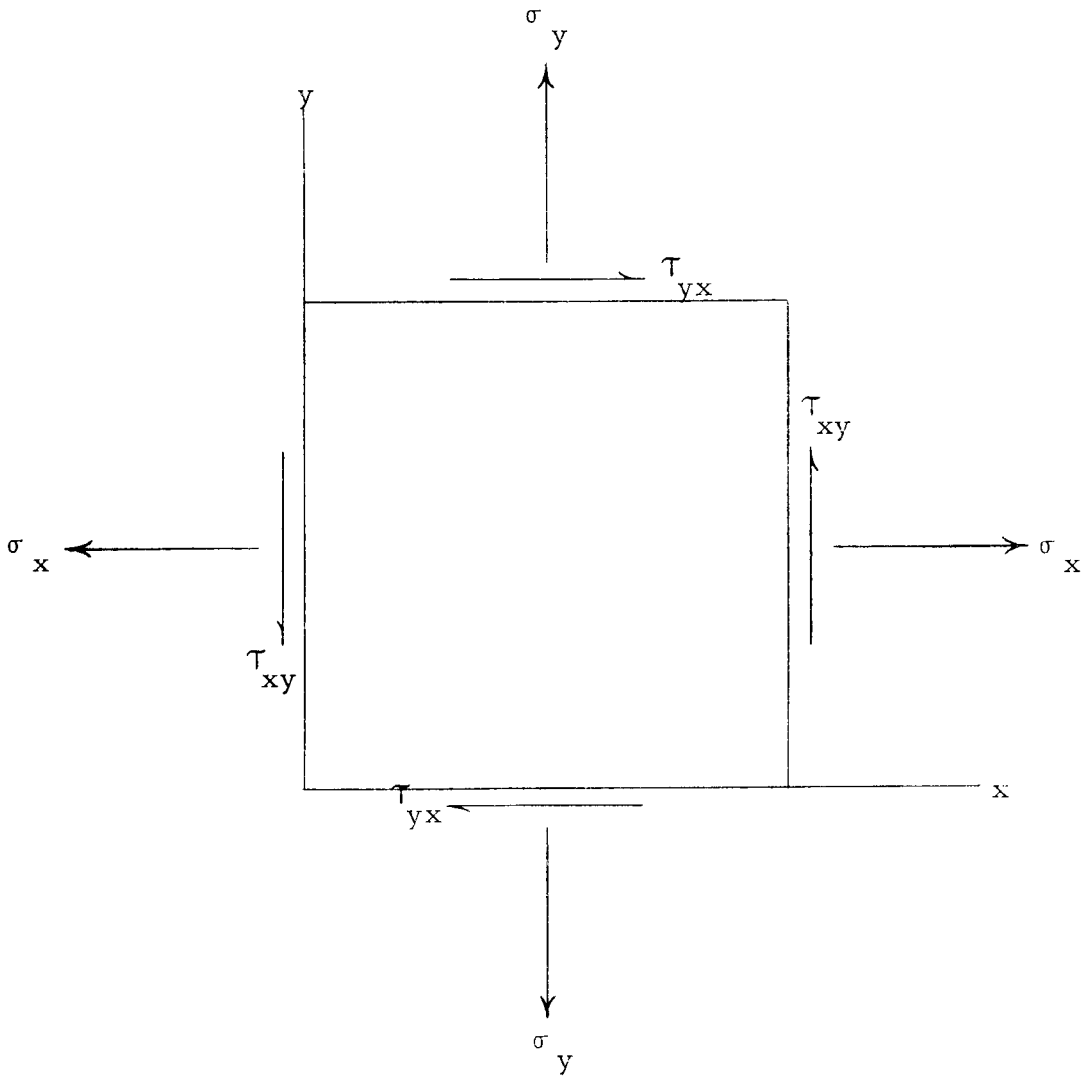

Figure 4. Stress-equilibrium orthogonal element.

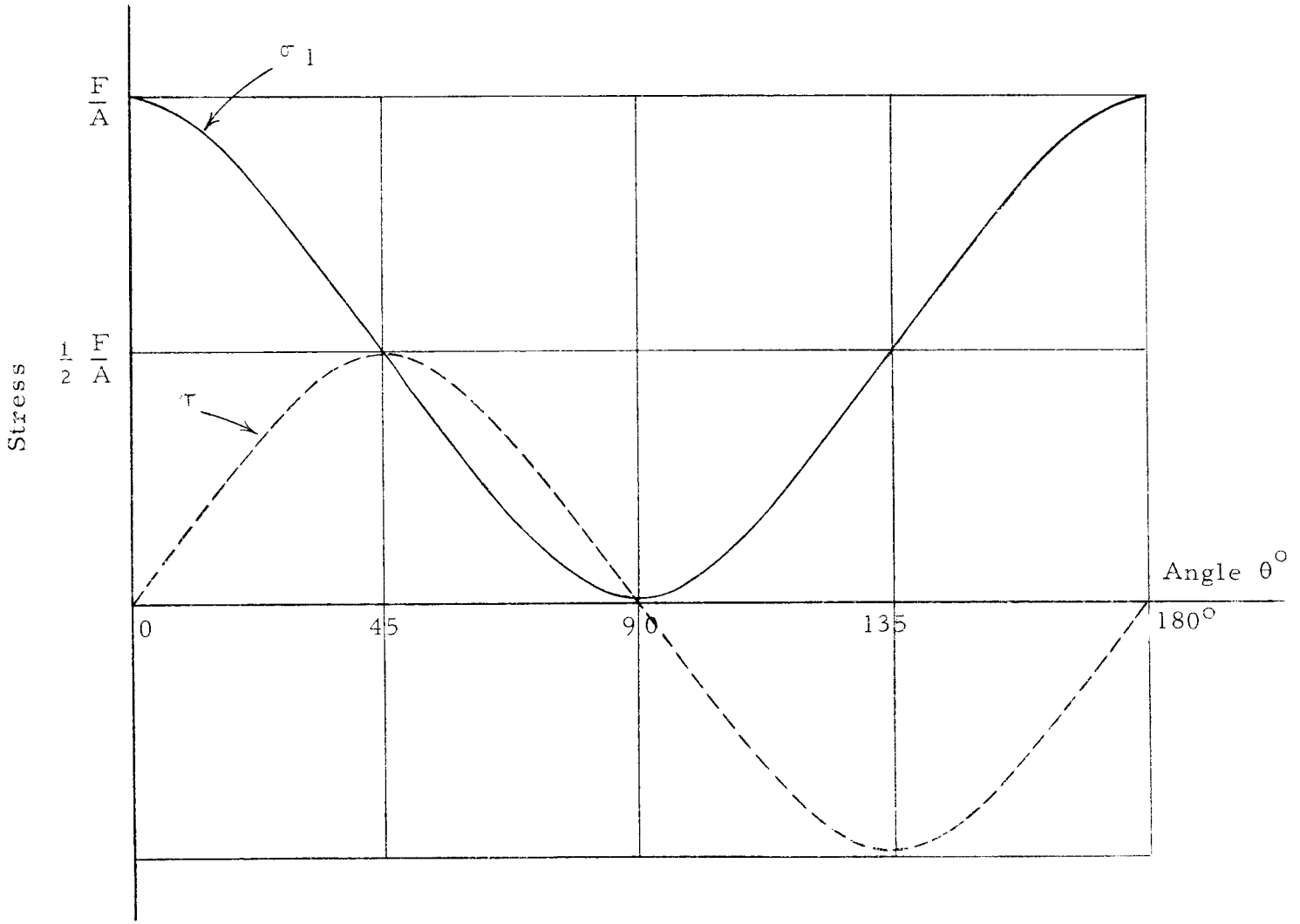

Figure 5. Normal and shearing stress curves.

value when θ is 0° or 180° and that τ is a maximum value when θ is 45° or 135°. Also, it may be seen that $\tau_{max} = \frac{1}{2}\sigma_{max}$ when the loading is simple tension or compression. The variation of the stresses over a two-dimensional stress field may also be expressed in a pair of differential equations known as the "equations of equilibrium". Using a rectangular set of axes, x-y, they are: (16, p. 7-8)

$$\frac{\partial \sigma_x}{\partial x} + \frac{\partial \tau_{xy}}{\partial y} + \overline{X} = 0$$

$$\frac{\partial \sigma_y}{\partial y} + \frac{\partial \tau_{xy}}{\partial x} + \overline{Y} = 0$$

where $\overline{X}$ and $\overline{Y}$ denote the components in the x and y directions of body-force which may often be neglected in comparison to the surface forces, as was mentioned earlier. Thus, the above equations may be simplified to (16, p. 6-8)

$$\frac{\partial \sigma_x}{\partial x} + \frac{\partial \tau_{xy}}{\partial y} = 0$$

$$\frac{\partial \sigma_y}{\partial y} + \frac{\partial \tau_{xy}}{\partial x} = 0$$

"When the relative position of points in a continuous body is altered, we say that the body is strained. The change in the

relative position of points is a deformation, and the study of deformations is the province of the analysis of strain" (17, p. 5). Deformation may take place in two basic geometric ways: First, a change in length and second, a change in angle. Such strains are called normal and shearing strain respectively. Normal strain may be defined as the change in length per unit original length of a straight line. This may be stated in the following expression (6, p. 25)

$$\epsilon = \underset{\Delta L \to 0}{\text{Limit}} \frac{\Delta \delta}{\Delta L}$$

where $\Delta \delta$ refers to the change in length of a segment initially ΔL long. From Hooke's Law it is realized that many materials behave in a manner that is approximately linear, that is the deformation is proportional to the applied load.

Uniaxial stress and strain are related by the expression (6, p. 32-34)

$$\frac{\text{Stress}}{\text{Strain}} = \text{a constant}$$

Hooke's Law for one-dimensional state of stress may be expressed as

$$\frac{\sigma}{\epsilon} = E$$

$$\frac{\tau}{\gamma} = G$$

for tension and shear respectively, where E and G are known as Young's modulus of elasticity in tension and shear respectively.

This is only a very brief discussion of elasticity in the two-dimensional case, but should be sufficient for this study of a photo-elastic load cell.

III. TWO-DIMENSIONAL PHOTOELASTICITY

Engineers are constantly trying to determine the stress on particular parts and it is for this purpose that the experimental technique known as photoelasticity was developed. Photoelasticity is used in conjunction with or in place of analytical methods where the member has a complicated geometric shape not readily solved by the mathematical methods.

Photoelasticity is a method of using light rays and optical techniques to study stresses and deformations in elastic bodies. This technique is based upon the unique property of certain transparent plastics being able to polarize light along the direction of principal stresses σ_1 and σ_2. These light waves also travel through the model with different velocities. When the light waves emerge there is a relative retardation which when viewed through a polariscope produces optical interference. This interference causes light and dark regions which are called fringes and which are a measure of the stress distribution in the model.

A circular polariscope will be used in this study. It employs circularly polarized light and consists of the following elements: light source, polarizer, first quarter wave plate, second quarter wave plate, and analyzer arranged as in Figure 6. There are four optical transformations being performed on the light in succession

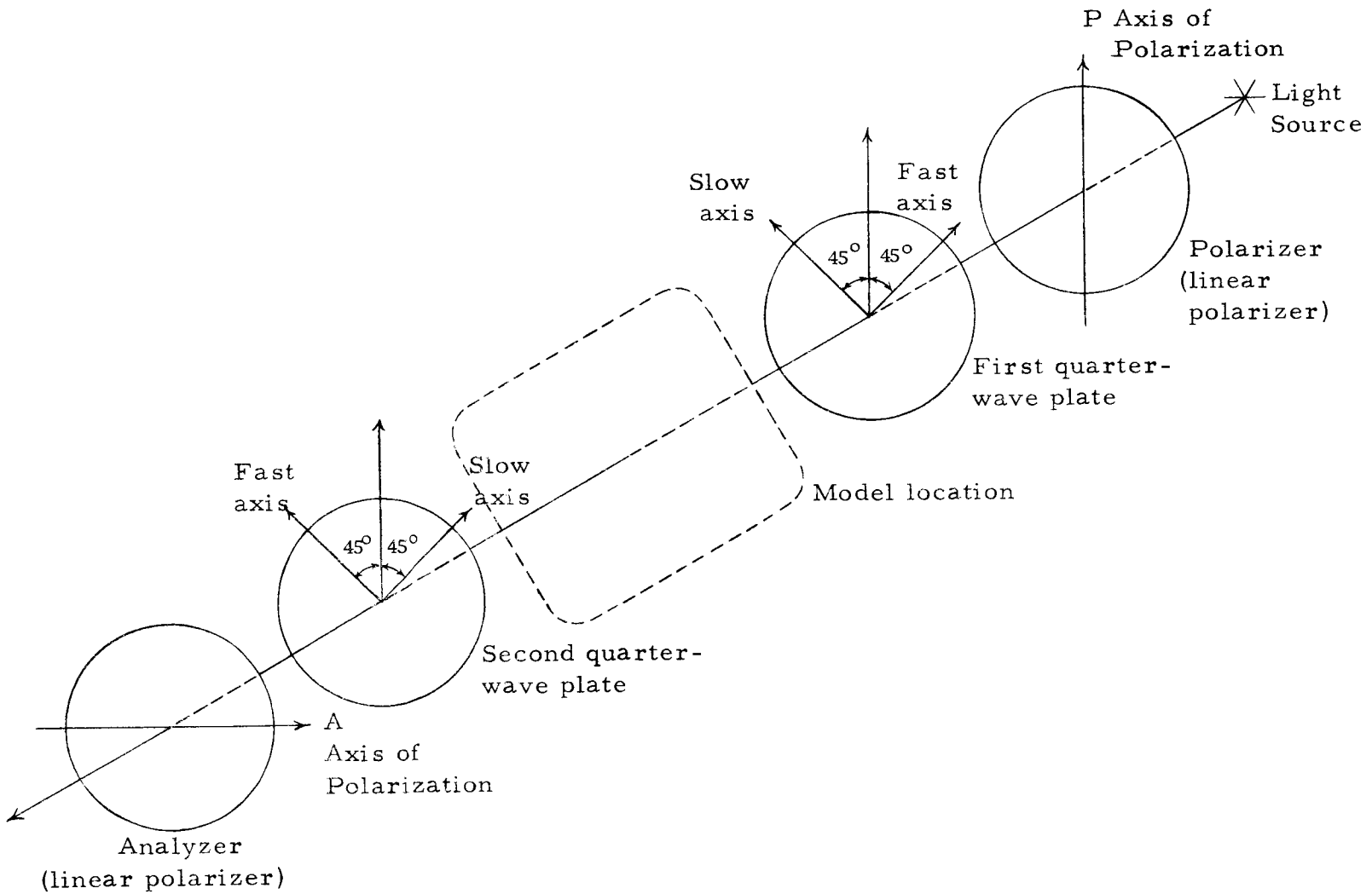

Figure 6. Arrangement of the optical elements in a circular polariscope.

on a circular polariscope. The polarizer converts the ordinary light into plane-polarized light. The quarter-wave plate is set at an angle of 45^{o} to the plane of polarization and transforms the preceding light into circularly polarized light. The model location is next and is followed by the second quarter wave plate set so that its fast axis is parallel to the slow axis of the first quarter wave plate. The light then emerges as plane-polarized light, which the analyzer may either block out or let through to give a dark or light field, respectively. Table 1 gives four possible arrangements of the elements in a circular polariscope.

Table 1. Arrangements of the Optical Elements in a Circular Polariscope

Arrangement	Quarter-wave plates	Polarizer and analyzer	Field
A	Crossed	Crossed	Dark
B	Crossed	Parallel	Light
C	Parallel	Crossed	Light
D	Parallel	Parallel	Dark

The theory of photoelasticity, or a description of what actually takes place when the photoelastic model is stressed in the field of polariscope, will now be discussed. This study will be concerned with the stress-optic law in two dimensions to arrive at the following equation: (3, p. 166-168)

$$\sigma_1 - \sigma_2 = \frac{Rf_\sigma}{h}$$

the term f_σ is the stress-optical coefficient or material fringe value in psi-in/fringe and is dependent upon the model material and the wavelength of the light employed, $f_\sigma = \frac{\lambda}{C}$. The model thickness is h. $R = \frac{\Delta}{2\pi}$ is the relative retardation and is known as the birefringence or isochromatic fringe order.

Consider a tensile specimen as in Figure 1 placed in a circular polariscope set for a dark field, meaning that extinction of light through the model occurs when the relative retardation is an integral number of wavelengths of the light employed (4, p. 57-59).

$$R = n\lambda \quad (n = \text{integer})$$

Maximum light occurs when the retardation is an odd number of half-wavelengths: (4, p. 57-59)

$$R = \frac{2n-1}{2}\lambda$$

If a plot of the light intensity vs. load is made of a tensile model a periodic function appears as in Figure 7. This curve may be derived by mathematical means to obtain the following relationship (16, p. 36)

$$I = a^2 \sin^2 \pi R = a^2 \left[\pi(\sigma_1 - \sigma_2)(C_1 - C_2) \frac{h}{\lambda} \right]$$

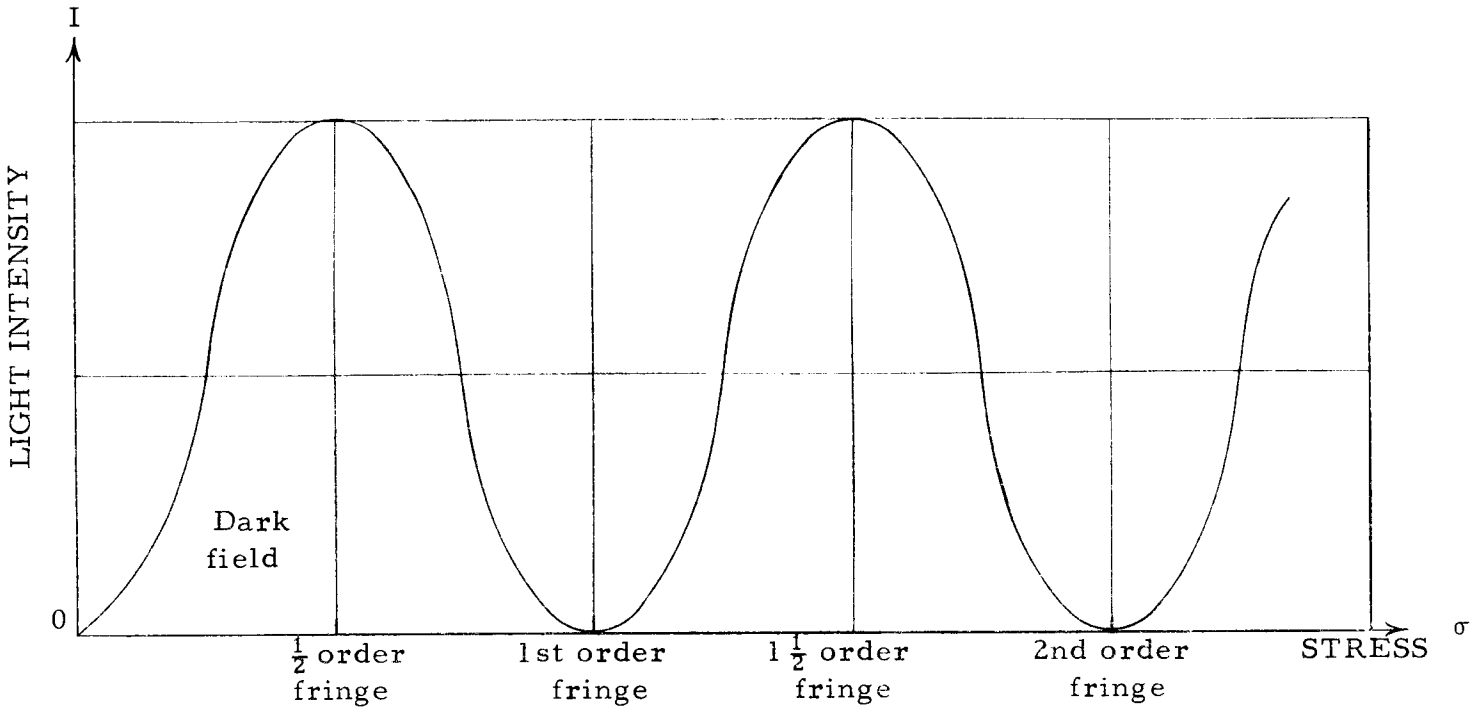

Figure 7. Intensity of light transmitted through a tensile specimen when the load is increased.

where

I = intensity of light

a = amplitude

R = the retardation

$\sigma_1 = \frac{F}{A}$ and $\sigma_2 = 0$ for simple tension

$C_1 - C_2$ = a constant for the model material

h = thickness of the model

This study will be concerned with the curve up to the first half order fringe.

IV. BASICS OF PHOTOCELLS

Four basic types of photosensors--photoemissive, photovoltaic, photoconductive junction type, and photoconductive balk effect--are available on the market today. This study will be concerned with the photoconductive balk effect cells which are normally made of cadmium sulfide (CdS) or cadmium selenide (CdSe). The photoconductor may be thought of as a variable resistance having an ohmic value that depends upon the intensity of light striking its sensitive surface. When light strikes the surface of the photoconductive cell, enough energy is expended upon the cell's covalent bond to cause an electron to be expelled, leaving a free electron and a hole. These holes, acting as a positive charge, travel toward the negative battery terminal. The larger the luminous flux on the photoconductive cell the more covalent bonds are broken which in turn decreases the resistance. In absolute darkness the resistance may be very high, in the order of 2,000,000 ohms. When stimulated by light its resistance may be as low as 10 ohms. For exact values of the light and dark resistance the manufacturer's data must be consulted. The conductivity of a photoconductive cell increases in a manner that is nearly linear with light intensity on a logarithmic plot as shown on Figure 8.

The photoconductive cell requires an external power source which may be an ordinary dry cell battery. A photoconductor without PN junction effects is non-polarized. This means that current

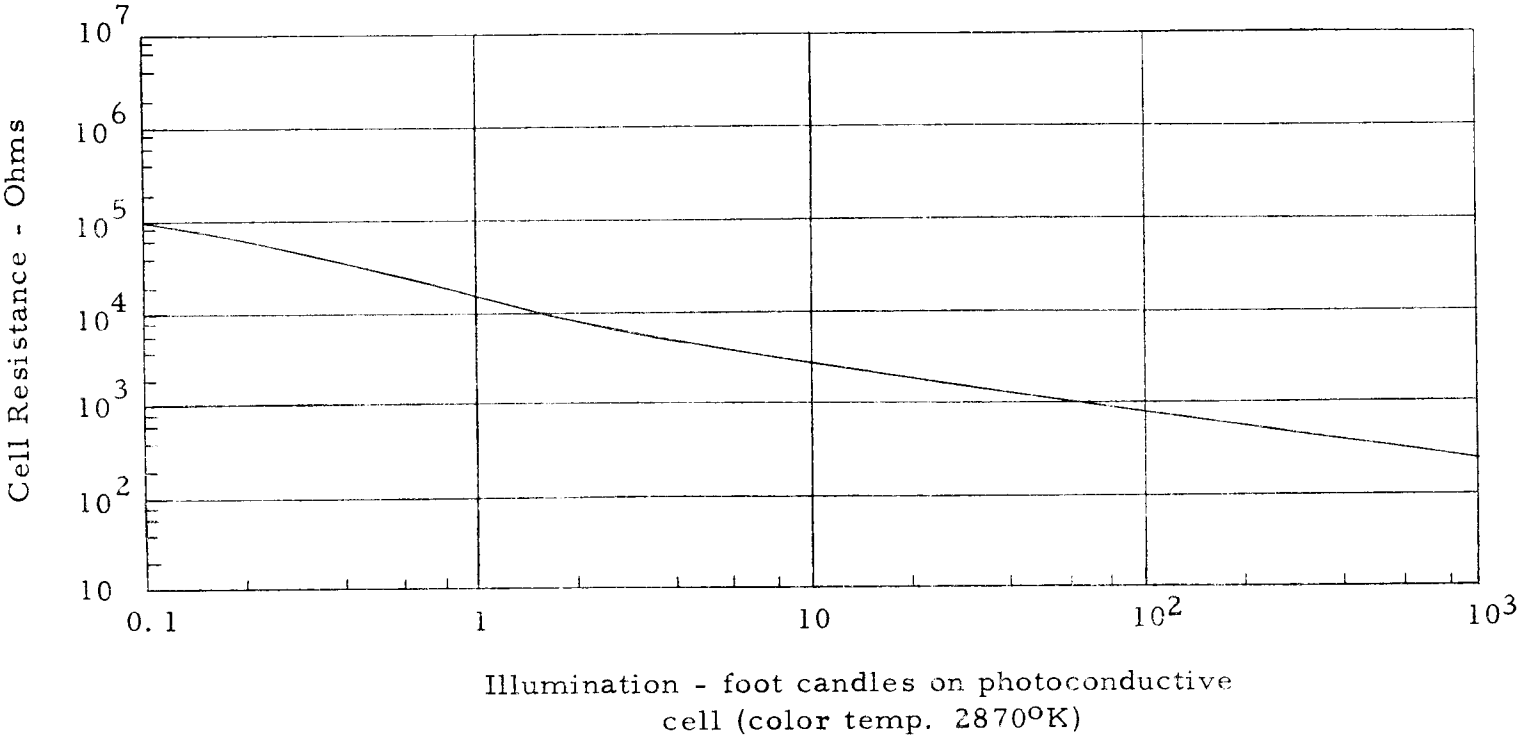

Figure 8. Intensity vs. resistance.

may flow through it in either direction equally well when the surface is illuminated.

The spectral response of the photoconductive cell must be considered in its application since its sensitivity is dependent on the wavelength of the incident light. A curve showing a photoconductive cell's sensitivity for various wavelengths of light is shown in Figure 9 (2). The speed of response of a cell is the time necessary for a change in illumination to produce a change in resistance. The time required by some photoconductive cells may be several minutes.

The presence of electron and hole trapping causes photoconductors to be susceptible to light history effects--variations of light sensitivity and response times with prior history of light and dark exposure (12, p. 73). The magnitude of this "light history effect" is dependent upon the difference between the previous and present light levels, and on the duration of previous and present exposures. This effect is a definite hindrance in making measurements of light intensity with photoconductive cells. Another problem encountered with photoconductive cells is the fact that they exhibit light fatigue effects, meaning their resistance increases with time under steady illumination.

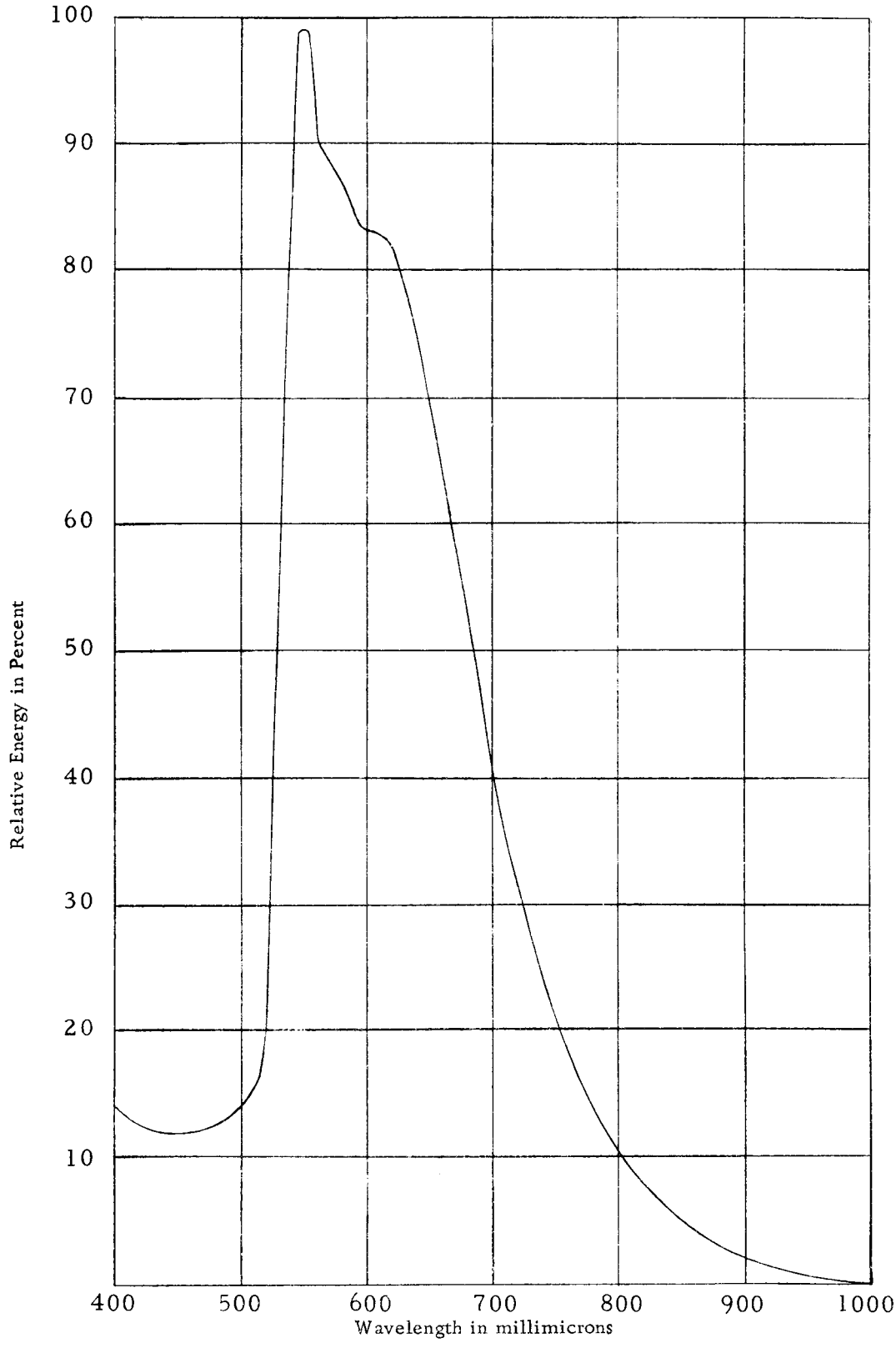

Figure 9. Spectral response of a photoconductor.

V. THE PHOTOELASTIC LOAD CELL

Design and Equipment

A General Electric Electroluminescent Lamp was selected for the light source for the miniature polariscope. The dimensions of the lamp are 2 x 2 x 1/32 inches. Its power consumption is 0.1 watt of a 120 volt, 60 cycle current to produce a green light. The spectral curve of the green lamp is shown in Figure 10. This curve may be shifted by using a current of different frequency (2).

Sheets of polaroid bonded to quarter wave plates were used in series to make up the miniature circular polariscope. The arrangement of the optical elements was such as to give a light field. Two photoconductive cells were mounted, one receiving its light through the polariscope and the other directly from the light source as shown in Figure 11.

The photoconductive cells were used in the circuit (Figure 12) with a Vacuum Tube Voltmeter (VTVM) as the readout equipment. A scale reading 0 to 50 was used on the meter. A full scale reading indicates approximately 1.5 volts difference between the two photoconductive cells. The voltage was obtained from two 6-volt dry-cell batteries connected in series. Several load cells of larger dimensions were built to test the theory against actual data before reducing the load cell to its final size of 2 x $2\frac{1}{2}$ x $1\frac{1}{4}$ inches.

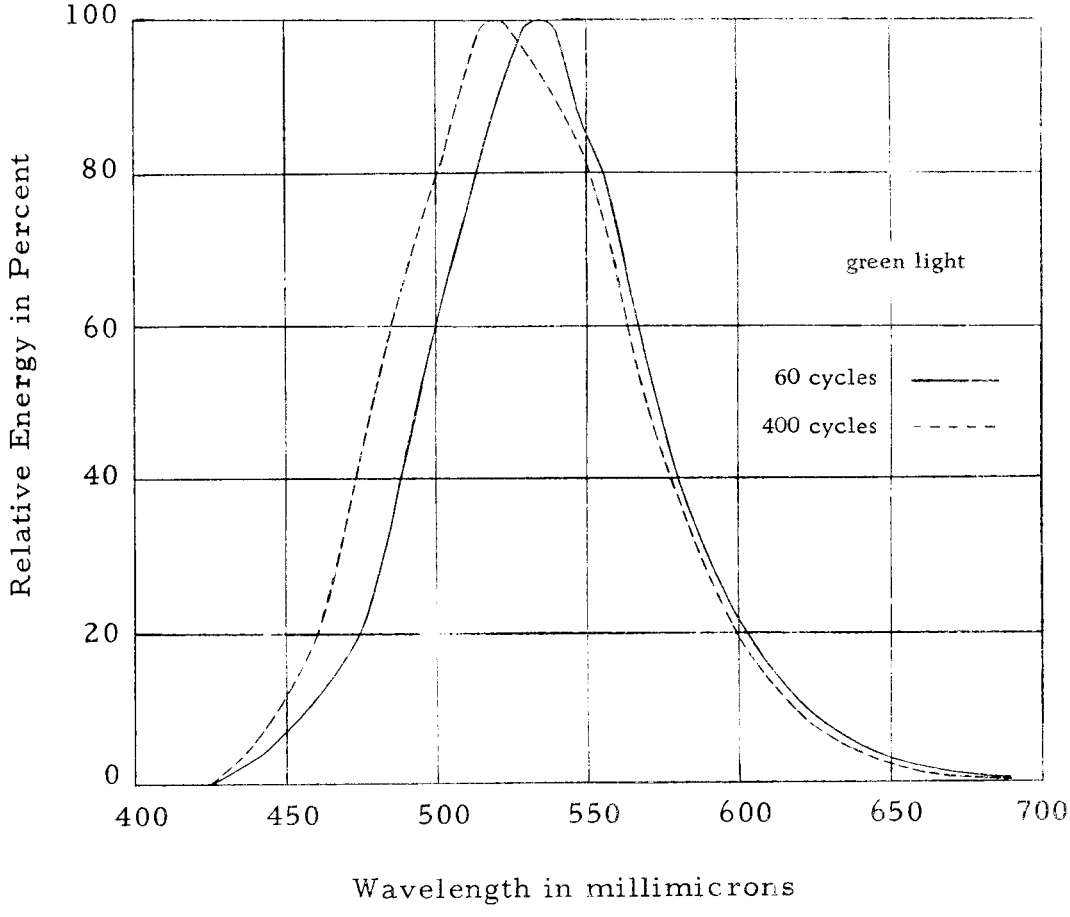

Figure 10. Spectral curve of light source.

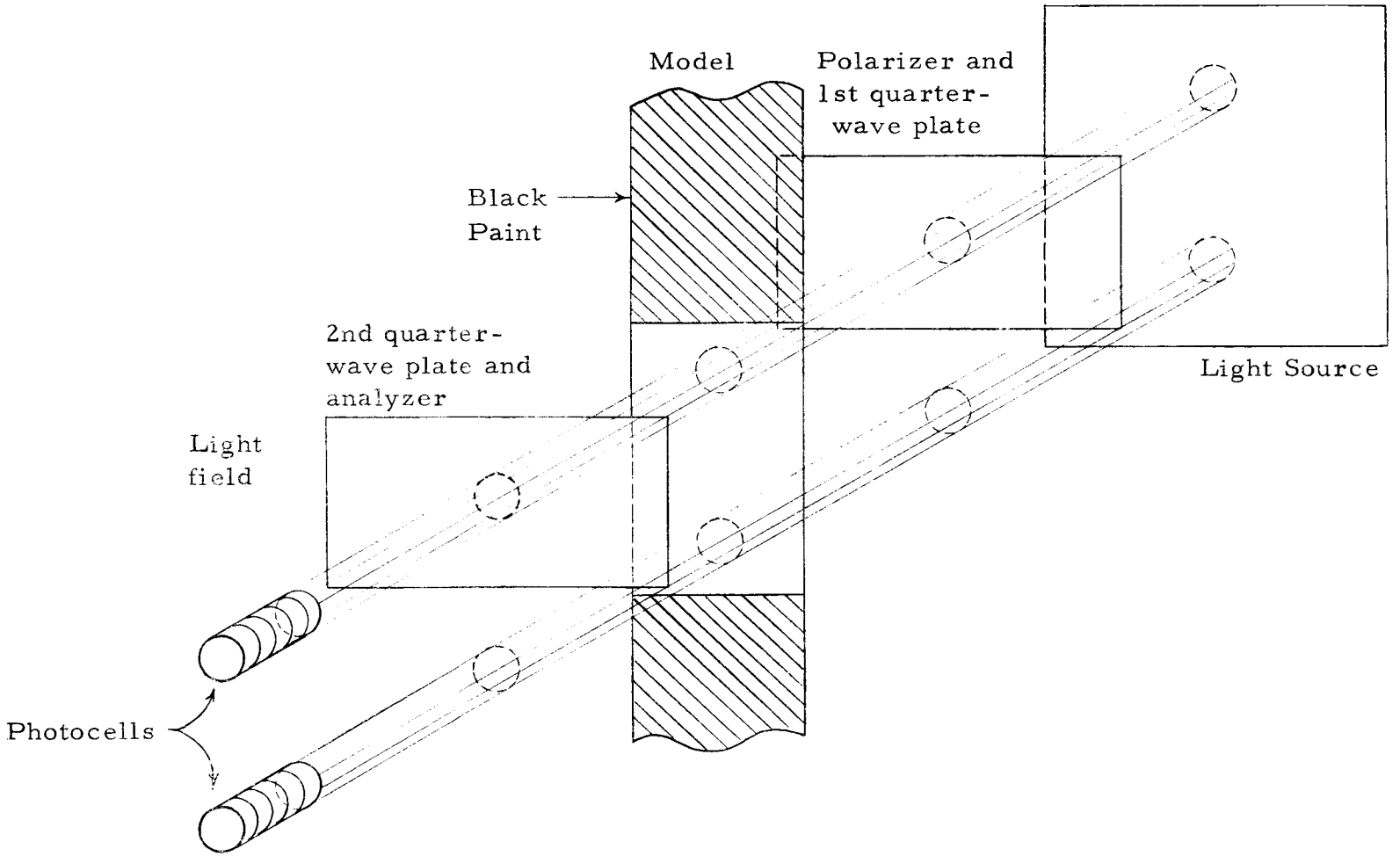

Figure 11. Arrangement of the load cell.

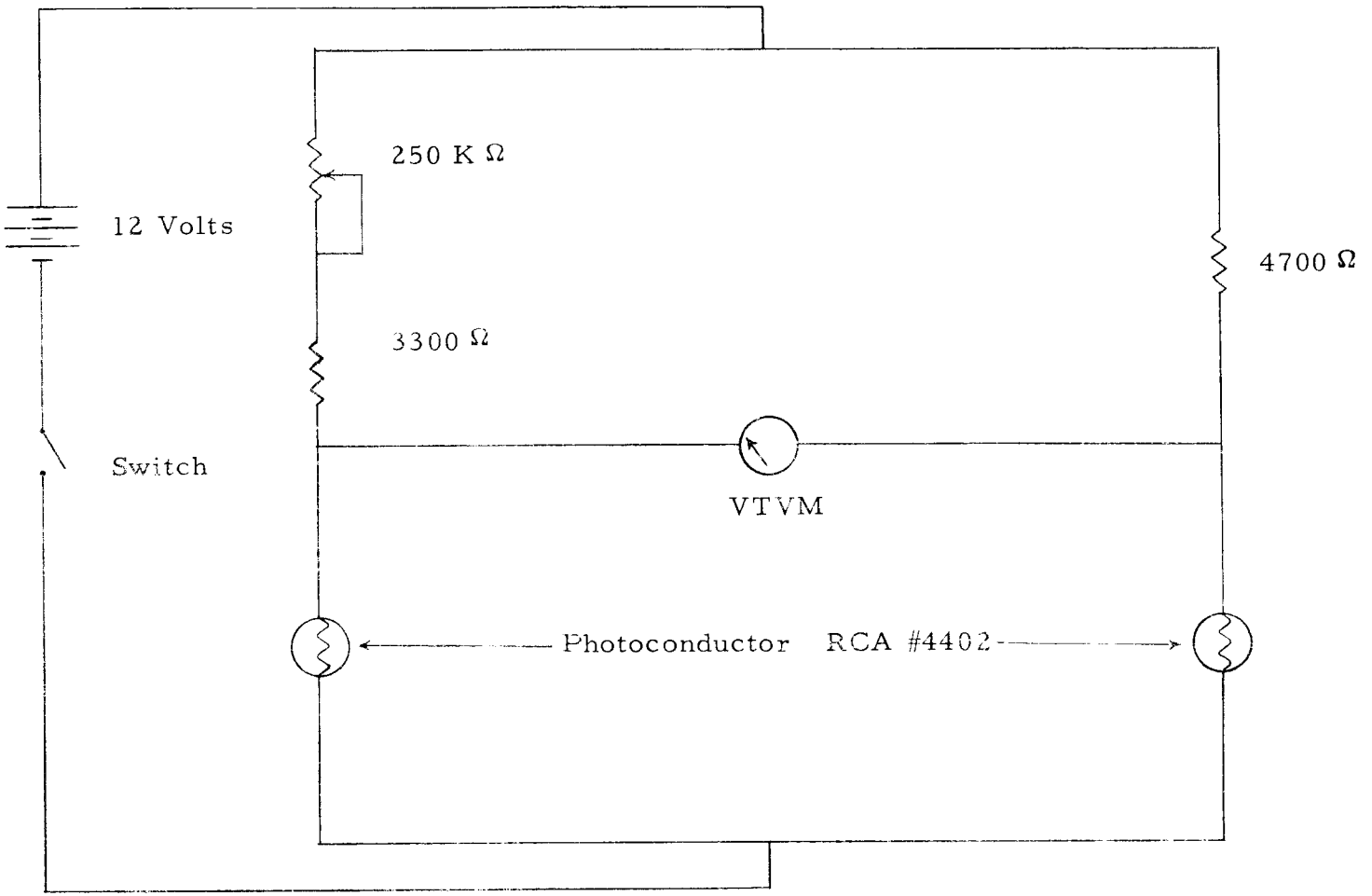

Figure 12. Circuit diagram for load cell.

The tensile model was painted flat black over its entire surface except for a small area, as shown in Figure 13. This area was to allow light to reach the photoconductive cells through the model. The model was placed in the load cell and a light seal between the model and load cell was put in place. This light seal was made from felt. The load cell is very sensitive to exterior light and any exterior light striking the photocells would give rise to false readings. The model installed in the load cell and ready for testing is shown in Figure 14.

The load cell was built with a rotational second quarter-wave plate and analyzer to enable one to align the circular polariscope for maximum light field before calibration. A "peek" hole was made for visual adjustment; however, the adjustment of the instrument was made from scale readings.

Calibration and Testing

Through calculations it was determined what load was required to bring in the first $\frac{1}{2}$ order fringe for a particular model; a somewhat smaller load was then selected for calibration purposes. This determined the load range of the load cell for the particular model. The calibration of the load cell for the $\frac{1}{2}$ inch wide CR-39 model was made to obtain a zero reading for no load and a full scale reading of 50 for a load of 4, 798 grams (10. 6 lbs.). The load cell was then

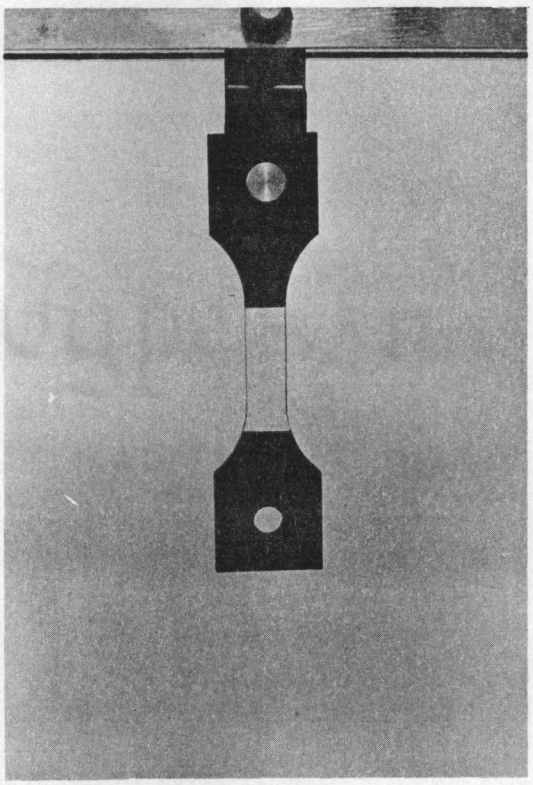

Figure 13. Tensile model used for testing.

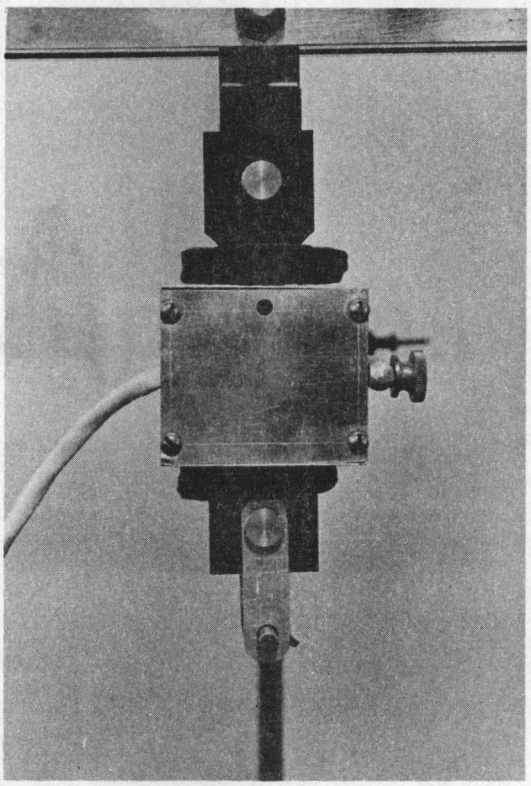

Figure 14. Tensile model installed in load cell.

progressively loaded and unloaded. The results of such a test are shown in Figure 15, giving a curve very similar to the first part of the curve seen previously in Figure 7. Thus, the experimental curve approximates the theoretical curve. However, one can see that at each end of the curve the slope decreases making accurate readings more difficult. Looking again at Figure 15, if the range of the load cell would exclude both ends of this curve, one would be left with an interval that is nearly linear. It was with this in mind that the actual testing of the load cell included a tare weight. By using a tare weight a portion of the curve at first was eliminated leaving one with a curve that was nearly linear.

Calibration of the load cell was now made to obtain a zero reading with the tare weight. A full scale reading of 50 was obtained for some loading that would eliminate the last part of the curve where the slope was decreasing. To calibrate: Zero the scale reading with the tare weight, apply dead weight of correct value for the particular model and adjust scale to read 50, check zero adjustment again. The load cell is now calibrated and ready for use. Using the load cell calibrated as described, two Columbia Resin CR-39 models were tested. The data collected over a period of several days with temperature variations of $72^{o}F$ to $80^{o}F$ is shown in Table II and Table III.

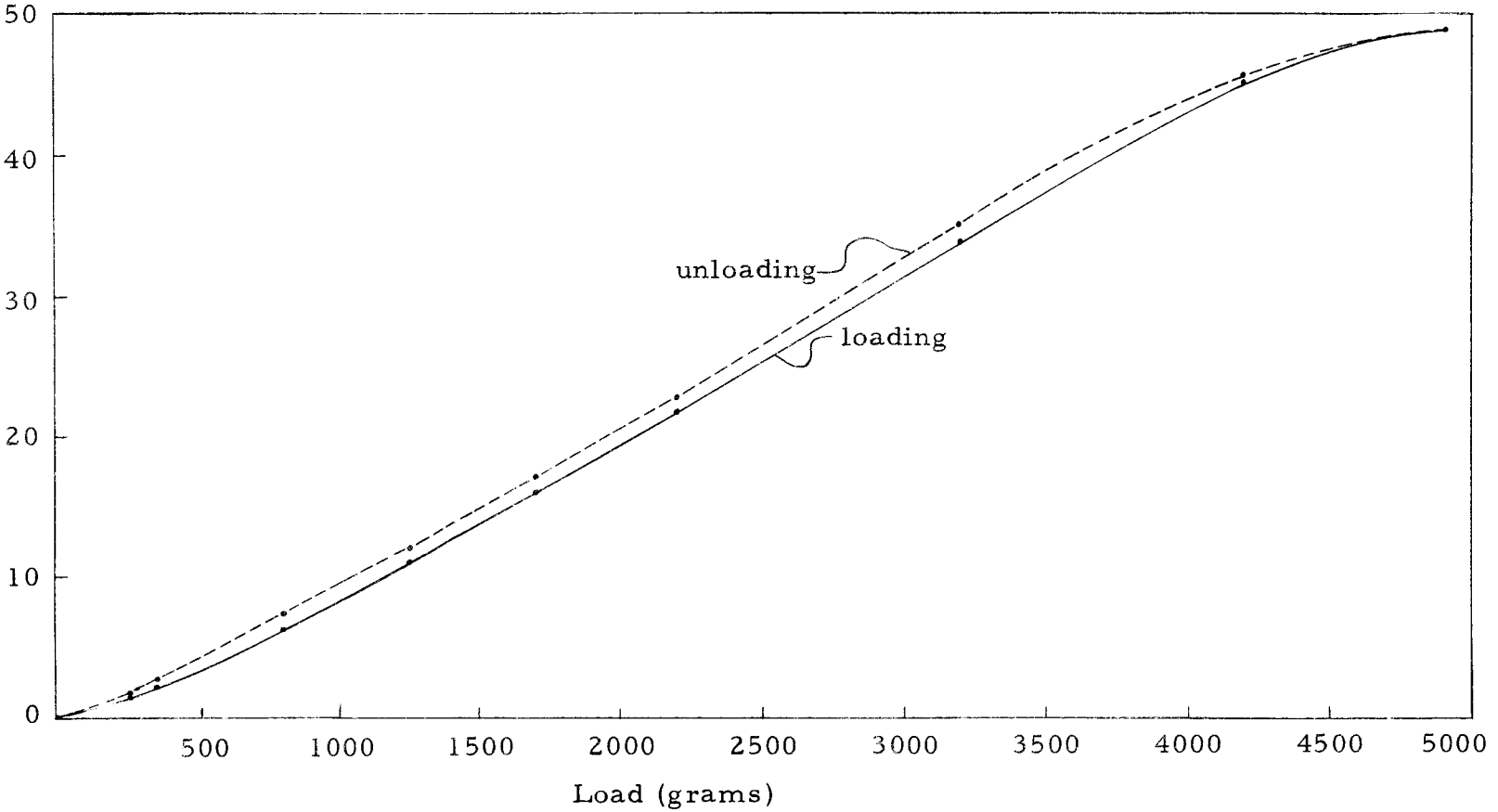

Figure 15. Load curve.

Table 2. CR-39 1" Wide Plastic Model, Temperature 72-82°F, Tare Weight 2492 grams

Load		Scale Reading											
		Progressive Loading						Progressive Unloading					
gms.	lbs.	Trial #1	#2	#3	#4	#5	#6	Trial #1	#2	#3	#4	#5	#6
0	0.0	0.0	0.0	0.0	0.0	0.0	0.0	0.6	0.3	- 0.2	0.0	- 0.1	0.2
453	1.0	0.8	0.7	0.7	0.7	0.9	0.8	1.8	1.4	0.7	1.2	0.9	1.2
906	2.0	1.8	1.6	1.7	1.9	1.8	1.9	3.0	2.6	2.0	2.5	2.3	2.4
1406	3.1	3.2	2.9	2.8	3.1	3.1	3.3	4.8	4.4	3.7	4.0	3.9	4.2
2406	5.3	6.5	6.2	6.3	6.7	6.6	7.0	8.2	8.0	7.3	7.8	7.8	7.9
3406	7.5	10.5	10.2	10.3	10.7	11.1	11.2	12.3	11.9	11.4	12.0	12.1	12.2
4406	9.7	14.9	14.7	14.8	15.1	15.4	15.5	16.8	16.4	16.3	16.8	16.7	17.0
6675	14.7	26.3	26.0	26.0	26.3	26.7	26.8	28.3	28.0	27.8	28.3	28.4	28.6
8944	19.7	38.6	38.5	38.1	38.8	38.6	38.6	40.1	39.9	39.3	40.2	39.6	39.8
11,213	24.7	49.7	50.0	48.5	49.8	48.9	49.1	49.7	50.0	48.5	49.8	48.9	49.1

Table 3. CR-39 1/2" Wide Plastic Model, Temperature 72-82°F, Tare Weight 258 grams

Load		Scale Reading											
		Progressive Loading						Progressive Unloading					
gms.	lbs.	Trial #1	#2	#3	#4	#5	#6	Trial #1	#2	#3	#4	#5	#6
0	0.0	0.0	0.0	0.0	0.0	0.0	0.0	0.0	0.1	0.2	0.2	0.0	0.1
90	0.2	0.3	0.5	0.5	0.4	0.7	0.7	0.5	1.0	1.1	1.0	0.9	1.1
543	1.2	4.4	4.7	4.7	4.4	5.0	4.4	5.1	5.6	5.8	5.9	5.5	6.1
996	2.2	9.1	9.1	9.3	9.8	9.8	9.7	10.1	10.6	10.7	10.7	10.4	11.1
1449	3.2	14.3	14.2	14.6	14.4	15.0	14.7	15.4	15.9	16.0	15.8	16.5	16.2
1949	4.3	20.1	20.1	20.1	20.0	21.0	20.1	21.8	21.9	22.3	21.5	22.7	21.8
2949	6.5	32.3	32.7	32.7	32.8	34.2	32.3	33.9	34.3	34.9	35.0	35.2	34.8
3949	8.7	43.3	44.2	44.0	43.6	45.6	43.7	44.1	44.9	45.2	44.6	46.0	44.7
4403	9.7	47.6	48.8	48.9	48.7	49.8	48.1	47.6	48.8	48.9	48.7	49.8	48.1

VI. RESULTS AND CONCLUSIONS

In the early stages of development of the load cell tests were made on the 1" plastic model to check its operation according to theory. Loading was applied to the model to produce up to $3\frac{1}{2}$ orders of fringes, producing a curve much like that shown in Figure 7. It was observed that the amplitude dropped slightly with increasing fringe order. Stressing a model to this extent required a load in the order of 300 pounds. A positive screw displacement loading frame was used to apply the load, but difficulties were encountered with this arrangement. Creep in the plastic model caused the load, as measured by a commercial load cell, to decrease gradually with time. This problem was quickly solved by using a dead weight loading frame, as shown in Figure 16. Another problem encountered was the determination of the load at a certain scale deflection. Unless one knew what order fringe was being approached, the load could not be determined. Also, at the inflection points on the curve accuracy would be greatly reduced. It is felt that further work in this area could be done using different readout equipment. The output signal could be integrated once or twice to produce a suitable curve. In Figure 17 the output signal has been integrated both once and twice to demonstrate how a more suitable curve could be obtained. Equipment necessary to do this, however, would greatly increase the cost

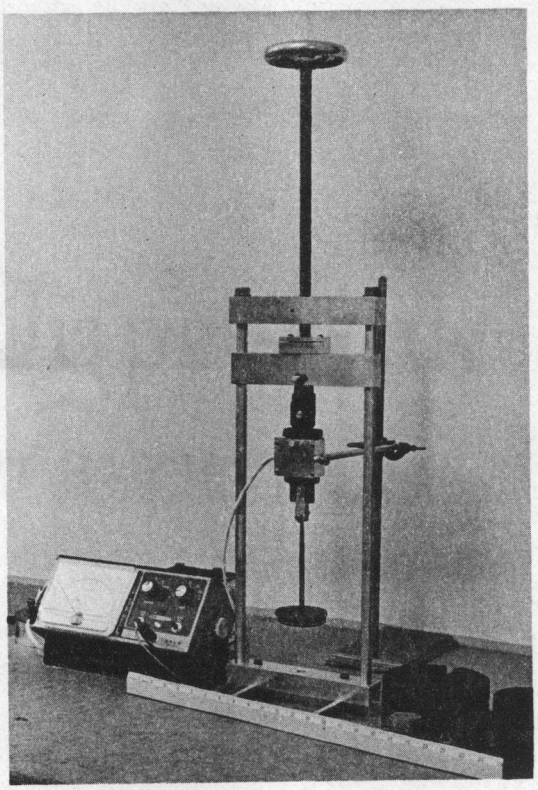

Figure 16. Dead weight loading frame.

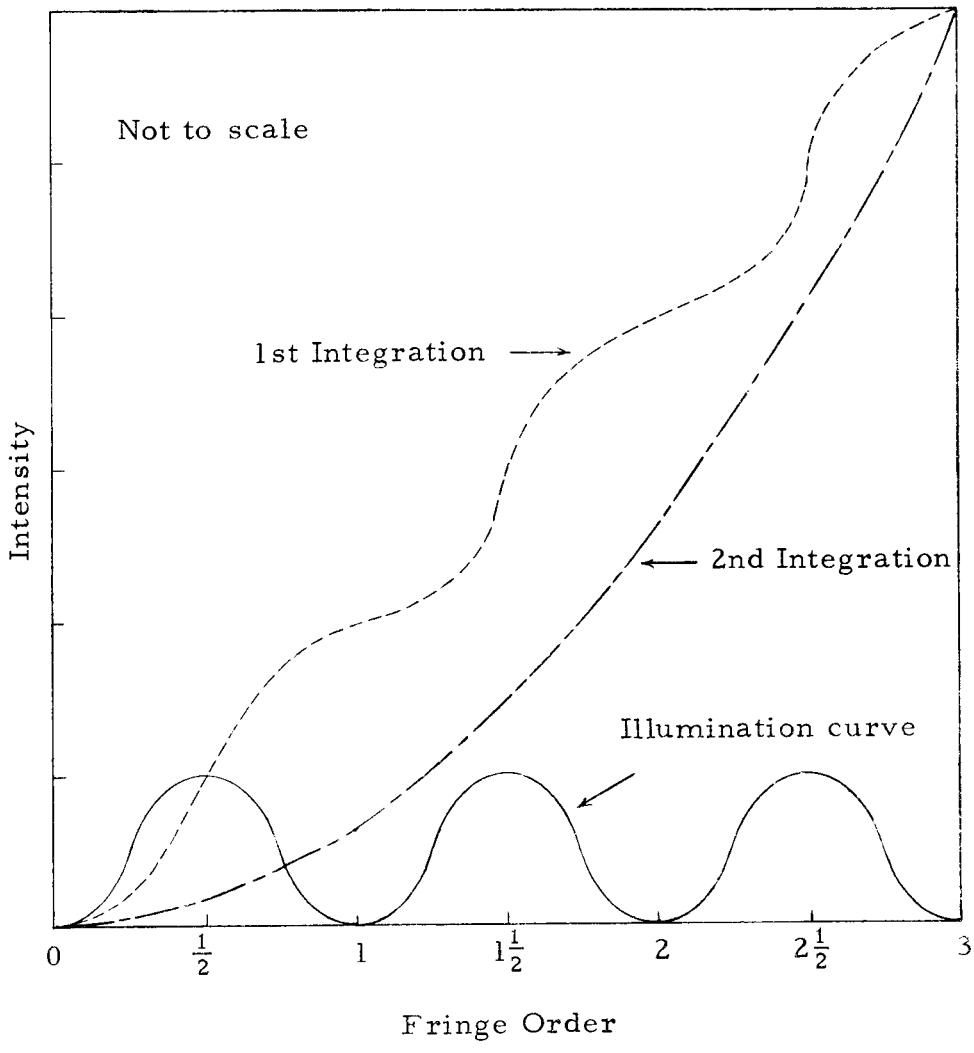

Figure 17. Integrated load curves.

of the load cell, but the range of the load cell would be expanded nearly five times by such a method. One further problem is the difficulty in obtaining a truly monochromatic light source. Further study in this area would likely solve these problems. Being interested at the present in a load cell with a maximum loading of under 50 pounds, many of the problems discussed above are not encountered.

Considering the data obtained from the load cell, some evaluation should be made. Whenever any data is collected the question as to how much data is needed must be answered. The data must then be presented in a meaningful manner that is useful to all concerned.

The determination of how many tests were needed was made by a statistical approach and it was found that about four trials were necessary for the desired accuracy (1, p. 95-96). The accuracy sought was determined by the VTVM being used. Its accuracy was ± 3% of full scale reading, thus limiting the load cell to this value. For increased reliability and accuracy 6 trials were made with each model.

Considering the data presented in Table II and Table III, a calibration curve as shown in Figure 18 and Figure 19 can be made. This is a record (graph) of the comparison of load cell output against standard test loads. There is a definite hysteresis loop in the curve which should be considered when using the load cell. From the

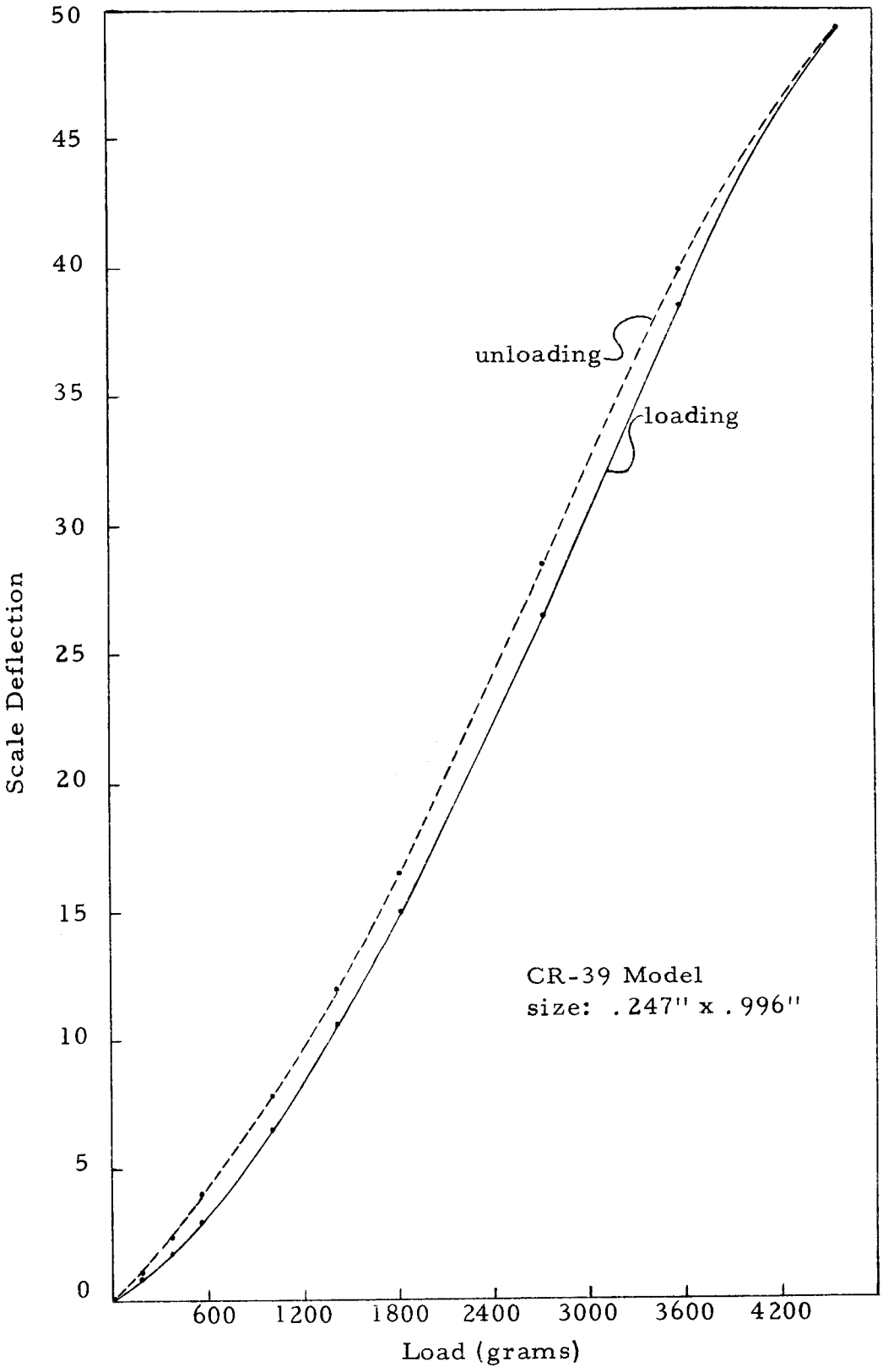

Figure 18. 1" model calibration curve.

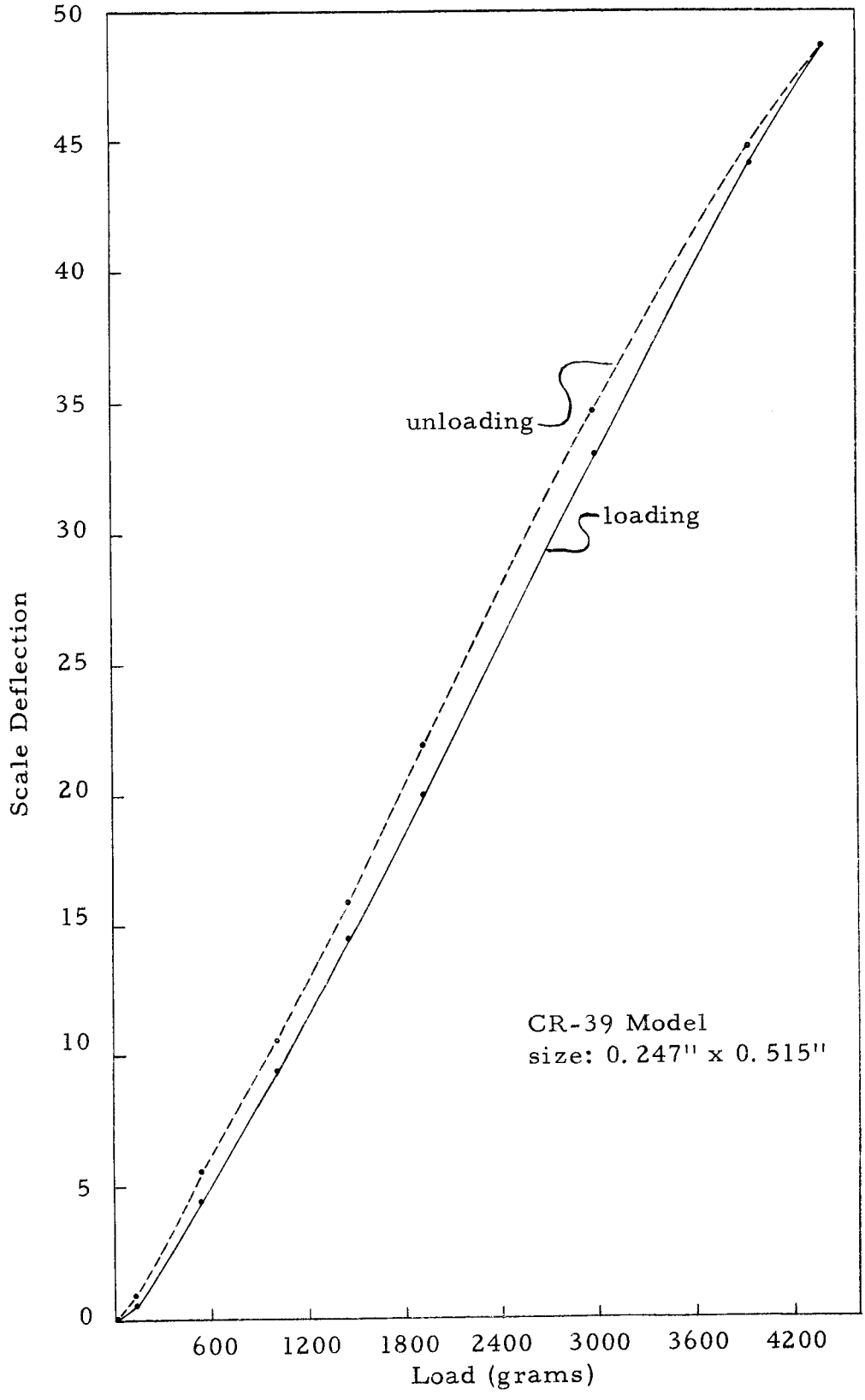

Figure 19. $\frac{1}{2}$" model calibration curve.

calibration curves it can be seen that the last $\frac{2}{3}$ of the curve is nearly linear. If desired, the tare load could be increased by a suitable amount to make an approximately linear curve; however, this would be at the expense of decreasing the range of the load cell.

The reason for the hysteresis loop can be satisfactorily explained as follows. There are two main factors which tend to make up the hysteresis loop, the model and the photoconductive cells. The model was made from CR-39, a plastic whose fringe order due to optical creep increases with time and would account for part of the hysteresis loop (4, p. 113-115). The photoconductive cells have several factors that would add together with the model to increase the size of the hysteresis loop. The speed of response may be such that the current has not reached a steady state condition since the change in illumination on the photoconductive cell took place. Photoconductive cells exhibit a "light history effect". This means that the instantaneous conductance of a cell is a function of the cell's previous exposure to light and the duration of this exposure. Finally, photoconductive cells exhibit light fatigue effects whereby their resistance increases with time under steady illumination (12).

These difficulties could add up to make a very sizeable hysteresis loop unless steps are taken to keep them at a minimum. All readings should not be taken until at least two minutes after the load change is made. The instrument should also be given a warm-up

period of approximately thirty minutes.

The "light history effect" could be virtually eliminated by keeping the photocells constantly in a light environment between measurements. For best results, a light level environment within the range of normal use should be chosen.

Some testing of the load cell in an oven was also made. The testing showed that the load cell could be used at higher temperatures ($160^{o}F$) but that the properties of the plastic changed at this higher temperature. This change in properties requires the load cell to be recalibrated. The operating range is considerably lowered by this higher temperature. A model used in the oven may be changed and cannot be assumed to have the same properties that it had before at room temperature. Its loading range was found to be somewhat lower than it was previously at room temperature. With these effects in mind it is reasonable to assume satisfactory results could be obtained with the load cell at elevated temperatures. Certain photoelastic materials exhibit different characteristics at elevated temperatures so the data for that material should be consulted.

Additional ranges of the load cell are possible by using different sized models as well as different materials. A urethane rubber model was tested and found to be useful in the range of 0 to 5 ounces. Extensive testing with this model was not carried on because of the difficulty encountered of sealing the load cell from external light.

Certainly this would be a problem quite easily solved if such a load range were desired. One method to try would be to not seal the light off but retain the same external lighting conditions when calibrating and using the photoelastic load cell.

To illustrate the potential of this load cell a tabulation of various photoelastic materials along with approximate load ranges are listed in Table 4.

Table 4. Useful Load Range for Various Photoelastic Materials.

Material	Stress fringe value (psi-in/fringe)	Approximate load ranges		
		$\frac{1}{2}$" Model	1" Model	$1\frac{1}{2}$" Model
Urethane Rubber Hysol 4485	0.90	0-2.7 oz.	0-5.4 oz.	0-8.1 oz.
Epoxy Resin Hysol 4290	60	0-11 lbs.	0-22.5 lbs.	0-34 lbs.
Columbia Resin CR-39	90	0-17 lbs.	0-34 lbs.	0-51 lbs.
Homolite 100	150	0-28 lbs.	0-56 lbs.	0-84 lbs.
Plexiglas	760	0-144 lbs.	0-285 lbs.	0-430 lbs.

The load ranges are just approximate values but give an indication of useful area. With this data in mind it can be seen that this load cell offers a very wide range of useful loadings while retaining high accuracy.

It is felt that this load cell is quite versatile, capable of being used either horizontally or vertically with numerous load ranges. The load cell, as shown in Figure 20, is not difficult to use and is compact in size. It may be easily calibrated by the use of dead weights prior to use and may be safely overloaded by 500% without damage. Among its other fine features is its surprising low cost. The load cell offers a quick, convenient and accurate means of measuring loads. All testing was of tensile loading but it was found that it would work equally well under compression as long as the load does not cause buckling of the model.

An approximate cost evaluation reveals its low cost compared to a commercial load cell of a similar single range. A commercially available load cell costs from $245 to $325. The readout equipment for these load cells may cost an additional $545 to $745. The readout equipment for the photoelastic load cell, the VTVM costs around $35, and the remaining materials can be purchased for less than $15, bringing the total cost to under $50 for the complete arrangement shown in Figure 21.

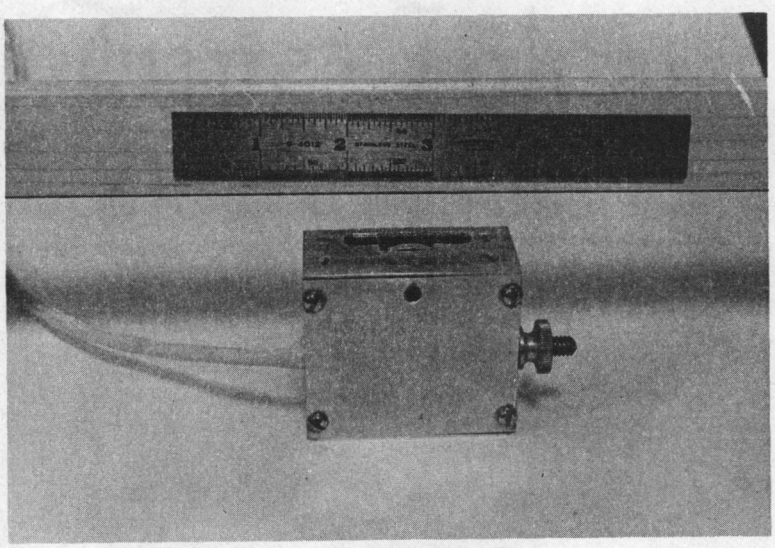

Figure 20. The load cell.

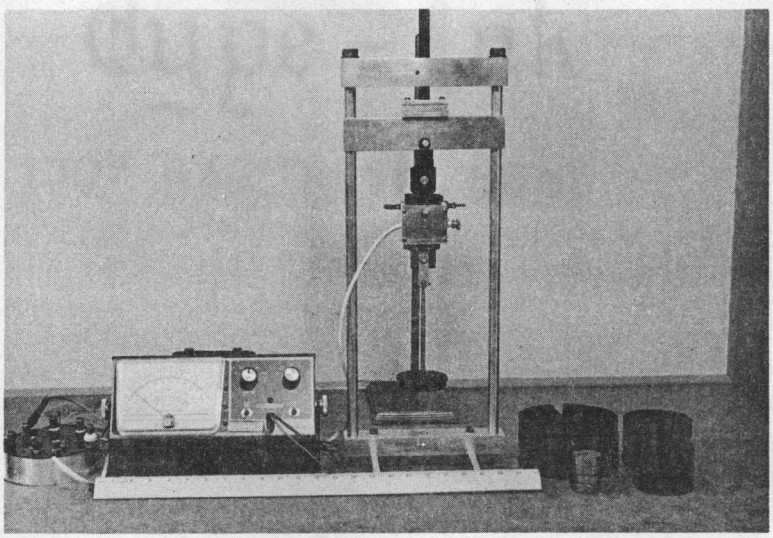

Figure 21. The complete load cell arrangement.

BIBLIOGRAPHY

1. Bryant, Edward C. Statistical analysis. New York, McGraw-Hill, 1960. 303p.

2. Clairex Corporation. Clairex photoconductive cell design manual. New York, 1966. 15p.

3. Dally, James W. and William F. Riley. Experimental stress analysis. New York, McGraw-Hill, 1965. 520p.

4. Durelli, A. J. and W. F. Riley. Introduction to photomechanics. Englewood Cliffs, N. J., Prentice-Hall, 1965. 402p.

5. Filon, L. N. G. A manual of photo-elasticity for engineers. London, Cambridge, 1936. 140p.

6. Frocht, Max Mark. Photoelasticity. Vol. 1. New York, Wiley, 1941. 411p.

7. General Electric Company. Miniature Lamp Department. Electroluminescent lamps. Syracuse, N. Y., n. d. 11p.

8. Green, A. E. and W. Zerna. Theoretical elasticity. London, Oxford, 1954. 442p.

9. Higdon, A., E. H. Ohlsen and W. B. Stiles. Mechanics of materials. New York, Wiley, 1960. 502p.

10. Hirsch, Werner Z. Introduction to modern statistics. New York, Macmillan, 1957. 421p.

11. Jessop, H. T. and F. C. Harris. Photoelasticity. New York, Dover, 1949. 184p.

12. Kaus, R. D. 1965 survey of commercial semiconductor photosensitive devices. Electronic Industries 24(7): 73-83. 1965.

13. Li, Jerome C. R. Statistical inference. Vol 2. Ann Arbor, Edwards, 1964. 575p.

14. Love, A. E. H. A treatise on the mathematical theory of elasticity. 4th ed. New York, Dover, 1944. 643p.

15. Mark, David. Phototubes and photocells. New York, Rider, 1956. 128p.

16. Society for Experimental Stress Analysis. Educational Committee. Manual on experimental stress analysis. Westport, Conn., 1965. 67p.

17. Sokolnikoff, I. S. Mathematical theory of elasticity. 2d ed. New York, McGraw-Hill, 1956. 476p.

18. Timoshenko, S. and J. N. Goodier. Theory of elasticity. 2d ed. New York, McGraw-Hill, 1951. 506p.

APPENDICES

APPENDIX A

SPECIFICATIONS FOR THE HEATHKIT SERVICE BENCH VACUUM TUBE VOLTMETER MODEL 1M-13

Electronic DC Voltmeter	
7 Ranges	0-1.5, 5, 15, 150, 500, 1500 volts full scale; up to 30,000 volts with accessory probe.
Input Resistance	11 megohm (1 megohm in probe) on all ranges; 1100 megohms with accessory probe.
Circuit	Balanced bridge (push-pull) usin twin triode.
Accuracy	± 3% of full scale.
Electronic AC Voltmeter	
7 Ranges	0-1.5, 5, 15, 50, 150, 500, 1500 rms scales (.353 of peak-to-peak).
Frequency Response (5 V range)	± db 25 cps to 1 mc (600 source, referred to 60 cps).
Circuit	Half-wave voltage doubler, using twin diode.
Accuracy	± 5% of full scale.
Input Resistance and Capacitance	1 megohm shunted by 40 μμf measured at input terminals (200 μμf at probe tip).
Electronic Ohmmeter	
7 Ranges	Scale with 10 center X1, X10, X100, X1000, X10K, X100K, X1MEG. Measures .1 to 1000 megohms with internal battery.
Meter	6", 200 μa movement, polystyrene case.
Probe	Combined AC-OHMS-DC switching probe, single jack input for probe and ground connections.
Dividers	1% precision type.
Tubes-Diode	1 - 12AU7, twin triode meter bridge. 1 - 6AL5, twin diode AC rectifier. 1 - Silicon diode power supply rectifier.
Battery	1-1/2 volt, size C flashlight cell.
Power Requirements	105-125 volts, 50/60 cps AC, 10 watts.
Cabinet Size and Finish	5" high x 12-11/16" wide x 4-3/4" deep (overall); charcoal gray
Net Weight	5 lbs.
Shipping Weight	6-1/2 lbs.

APPENDIX B

SPECIFICATIONS FOR THE PHOTOCONDUCTIVE CELL

In this study two Radio Corp. of America (RCA) #4402 photoconductors were used. They were of the Cadmium Sulfide (CdS) material. The followings lists some of the specifications for this photoconductor:

Spectral Response;	Spectral limits (10% points)	0. 33-0. 74 micron
	Sensitivity peak	0. 58 micron
Physical Dimensions;	Diameter	0. 29 inches
	Depth	0. 58 inches
	Sensitive area	0. 049 sq. in.
Maximum Ratings;	Voltage between terminals, DC or AC	300 volts
	Power dissipation	0. 05 watt
	Photocurrent	5 ma